ISSN 0915-633X

NATIONAL INSTITUTE FOR FUSION SCIENCE

He-like Spectra Through Charge Exchange Processes in Tokamak Plasmas

T. Kato, K. Masai, T. Fujimoto, F. Koike, E. Källne,
E. S. Marmar and J. E. Rice

(Received – Dec. 12, 1990)

NIFS-69 Jan. 1991

RESEARCH REPORT
NIFS Series

NAGOYA, JAPAN

Abstract

Population mechanisms and cascade effects due to charge exchange processes between hydrogen- like ions and neutral hydrogen are investigated for helium-like ions in tokamaks by using a collisional radiative model. Dependences of charge exchange cross sections on both the principal and angular momentum quantum numbers n, ℓ are estimated from the observed spectra.

Key words

charge exchange process, n - ℓ distribution, population inversion, tokamak plasma, Ar^{16+} ions

He-like Spectra through Charge Exchange Processes in Tokamak Plasmas

T. Kato, K. Masai,
National Institute for Fusion Science, Nagoya 464-01, Japan

T. Fujimoto ,
Dep. of Engineering Science, Kyoto University, Kyoto 606,Japan

F. Koike,
School of Medicine, Kitasato University, Kanagawa 228, Japan

E. Källne ,
Department of Physics I, The Royal Institute of Technology,
S 10044 Stockholm, Sweden

E.S. Marmar and J.E. Rice
Plasma Fusion Center, Massachusetts Institute of Technology,
Cambridge,Masachusetts 02139, U.S.A.

1. Introduction

X-ray spectral lines associated with He-like ions have been observed for many tokamak plasmas, and their emission intensities have been discussed in terms of population mechanisms of excited states. In quantitative analysis of the spectra, ionization, excitation and recombination processes have been taken into consideration, but the charge exchange process has generally been ignored except for the case of neutral beam injection. Although the influence of the charge exchange process on the spectra is mentioned in the discussion of some experiments, only a qualitative account is presented. The charge exchange process could be important for He-like spectral lines in relation to the population mechanism following the electron capture into higher energy levels. We investigate this process using a collisional radiative model which includes all the possible angular momentum ℓ state sublevels up to the principle quantum number $n = 40$ of He-like system. We apply this model to the spectra obtained from Alcator-C tokamak plasmas [1,2,3] and derive the $n - \ell$ distribution of charge exchange cross sections.

2. X-ray spectra from the Alcator C tokamak

In this section we summarize the results of the experiments on the Alcator-C tokamak[1,2,3]. Our investigation described in the subsequent sections is based on these observations.

Space-resolved X-ray spectra of Ar^{16+} (He-like) were observed from Alcator-C Tokamak plasmas with Ar gas puffing. In Fig.1, reproduced from Ref.1, spectral lines from n = 2 to n = 1 transitions, w ($1s^2\ ^1S - 1s2p\ ^1P$), x ($1s^2\ ^1S - 1s2p\ ^3P_2$), y ($1s^2\ ^1S - 1s2p\ ^3P_1$) and z ($1s^2\ ^1S - 1s2s\ ^3S$), are shown for three different lines of sight through the plasma; these are at the center (a), and through the points of d = 8.3 (b) and 11.3 cm (c) off from the center, where d is the shortest distance to the chord of observation from the plasma axis. The limiter radius was 16.5 cm. One can see a drastic change in the spectra from the central chord to the outer ones. The relative intensities of the forbidden line I_z and the intercombination lines I_x and I_y to the resonance line intensity I_w: I_z/I_w, I_x/I_w and I_y/I_w, increase remarkably towards the outer chords. This relative enhancement could be accounted for by an increasing contribution from radiative recombination to the excited-level populations[3] towards the outer region. The spectrum in Fig.1(c), however, cannot be accounted for only by the radiative recombination process. The observed intensity ratio of $I_z/(I_x + I_y) = 0.9 \pm 0.2$, is considerably smaller than the value 1.5 expected from radiative recombination. A possible interpretation is that a charge exchange process between Ar^{17+}(H-like) and hydrogen atoms dominates the population of highly excited states, and that the relative enhancement of the intercombination lines results through cascades[1].

X-ray spectra of the transitions $1s^2$ - 1snp with $3 \leq n \leq \infty$ were also obtained.[2] Fig.2 shows the observed spectra with $7 \leq n \leq 13$ through the three chords d = 3.9 cm (a), 8.0 cm (b) and 13.5 cm (c). As seen in Fig.2, the transitions from n = 9 and n = 10 are enhanced relatively to those from n = 7 and 8 towards the outer chord. This is regarded as a clear evidence of charge exchange recombination between Ar^{17+} and neutral hydrogen in the ground state into the levels of n = 9 and 10 [2,3]. Another observed spectrum corresponding to the highly excited states $n \geq 10$ is shown in Fig.3, which was obtained for d = 8.3 - 13.2 cm. The spectrum in Fig.3 shows a broad feature from 3.01 to 3.02 A. A peak at around 3.013A corresponds to the transitions from $n \approx 27$ and the shoulder near 3.018 A to the transition from $n \approx 18$. These enhancements are attributed to electron capture from hydrogen atoms in the excited states with the principlal quantum number n_i = 3 and 2, respectively[2,9].

3. Effect of cascades following charge exchange recombination

We construct a collisional radiative model for He-like ions where the levels of $n \leq 40$ are resolved with different angular momentum ℓ . The total number of levels considered is 1641. In the present study, we include the charge exchange process,

$$Ar^{17+}(1s) + H(n_i) \rightarrow Ar^{16+}(1sn\ell) + H^+ \qquad (1)$$

as an additional population mechanism of excited levels. Adjusting the magnitude of the charge exchange cross sections,

we try to fit the calculated line intensities to the experimental data described in the preceeding section.

i) The n - ℓ distribution of the charge exchange cross section

Abramov et al.[5] obtained an ℓ distribution $W_{n\ell}$ for the charge exchange process based on the Landau-Zener theory with a modification including rotational coupling effects,

$$W_{n\ell} = (2\ell + 1)[(n-1)!]^2/[(n+\ell)!(n-1-\ell)!]. \quad (2)$$

The cross section takes its maximum value 7 x 10^{-15}cm^2 at around n = 9 for H + Ar^{q+} collisions with q = 17.[6] The ℓ distribution in eq.(2) for n = 9 is shown in Fig.4 by the dot-dashed line. The n-ℓ distribution for the charge transfer cross section for H + Si^{q+} collisions was calculated in Ref.7 with atomic - orbital basis. Their distribution for collisions between H-like silicon (Si^{13+}) and H atoms at 350 eV increases with increasing the ℓ value similarlly to the statistical weight, as shown in Fig.4 by dashed lines. A continuous - energy state model is proposed for charge transfer processes by Koike,[8] whose method is applied to the n-ℓ distribution of the process given by eq.(1). The cross section at 350 eV takes its maximum at around ℓ = 3 from his results as indicated in Fig.4 by solid lines for n = 9 and n = 10. Three different theories give quite different distributions. The ℓ distribution for n = 10 of radiative recombination σ_r at 100 eV is shown in the

upper part of Fig.4 for comparison. The ϱ-value that gives the maximum of σ_r increases as the electron energy decreases and as the principal quantum number n increases, but the value does not exceed $\varrho = 4$.

ii)Contribution of radiative recombination by electron collisions

The intensity I_{10} in Fig.3 is much stronger than those of I_{13} and I_{14}, where I_n means the line intensity of the $1s^2$ - 1snp transition. Due to convective transport in the plasma, a considerable fraction of highly ionized ions may exist even in the outer regions with the temperature as low as ~300 eV. Ar^{16+} spectra observed from such a plasma exhibit typical characteristics of recombination.[3,4] In fact, as seen in Fig.3, the recombination continuum is detected at wavelengths shorter than 3.0088 A which is the ionization limit of the $1s^2$ state. We assign the intensity at I_{13} location as due to radiative recombination. Then we estimate the upper limit of the electron temperatue T_e to be about 500 eV from the observed intensity ratio of $I_{13}/ J_{cont} \lesssim 2.8 \times 10^{-4}$ Å, where J_{cont} represents the continuum intensity in units of photons / Å. The continuum level is taken from the short wavelength edge of the spectrum. The value 500 eV is reasonable for the electron temperature around r = 11 cm. From the intensity of I_{13}, the contribution of radiative recombination to the line

intensities, $I_{10} - I_{12}$, and $I_{n \geq 15}$ is estimated . The resulting intensities are much lower than those observed. On the other hand, the contribution of electron excitation is estimated to be negligibly small since the electron temperature is much lower than the excitation energies.

Thus, the intensity I_{10} is understood to be dominated by direct electron capture through charge exchange with neutral hydrogen. The intensities I_{10} and J_{cont} are written as

$$I_{10} = N(Ar^{17+})N_H(1)\langle\sigma_{cx}(10p\ ^1P)v\rangle \qquad (3)$$

$$J_{cont.} = N(Ar^{17+})N_e\alpha_{f-b}(\lambda=3\mathring{A}) \qquad (4)$$

where

$$\alpha_{f-b}(\lambda(A)) = 3.97\times10^{-12}\exp(I_z-12.4/\lambda)\lambda^{-1}(kT_e(keV))^{-3/2}d\lambda$$
$$(photons/\mathring{A})\ cm^3\ s^{-1} \qquad (5)$$

is the radiative recombination rate coefficient at wavelength $\lambda(\mathring{A})$, T_e the electron temperature, $\sigma_{cx}(10p\ ^1P)$ is the charge exchange cross section to the $1s10p\ ^1P$ state, v the velocity of Ar^{17+} relative to the hydrogen atoms, and N_e and N_H (1) the densities of the electron and the neutral hydrogen in the ground state, respectively. Then the following relation is derived from the observed value $I_{10}/J_{cont}d\lambda = 8$ where $d\lambda = 1.79\times10^{-3}\mathring{A}$,

$$\sigma_{cx}(10p\ ^1P)v\ N_H(1)/N_e = 5.0\ x\ 10^{-14}\ cm^{-3}s\ . \qquad (6)$$

For the values of $N_e = 5 \times 10^{13}$ cm^{-3}, $N_H(1) = 10^9$ cm^{-3} and $v = 2.5 \times 10^7$ cm/s ($T_i = 350$ eV), the cross section $\sigma(10p\ ^1P)$ is estimated to be $1.0 \times 10^{-16} cm^2$. Assuming the statistical distribution for singlet and triplet states, we obtain $\sigma(10p) = 4.0 \times 10^{-16}$ cm^2 which is consistent with the theoretical value[8] (see Fig.4). But this value changes according to the estimate of the densities of electron and neutral hydrogen as well as of the ion temperature. We discuss only the relative values for the cross section later on.

iii) Cascade effect of ℓ distribution on the spectra with $7 \leq n \leq 12$

We now turn to the lines from n = 7 - 9 in Fig. 2(c), where the electron termperature is estimated to be about 290 eV. The intensities $I_{n = 7-9}$ are also much stronger than $I_{n \geq 11}$, and we assume that this enhancement is attributed to charge exchange recombination as in the case of I_{10}. However in the present case, it is unlikely that these upper levels are populated entirely by direct capture. Rather, the fact that the intensity I_7 is higher than I_8 strongly suggests some contribution of cascades from n = 10 and/or 9.

In Fig.5 we show the calculated spectra including charge exchange recombination for the capture into the 10ℓ selected state ($\ell = 1,2,....$) in order to see the effect of the ℓ distribution on the spectra. The charge exchange recombination rate coefficient is tentatively assumed to be $\alpha_{cx} = 5.2 \times 10^{-6}$

$cm^3 s^{-1}$, which is much larger than that of the radiative recombination rate by ten orders of magnitude, in order to see the effect by charge exchange recombination. The distribution ratio of the singlet state to the triplet one is assumed to be 1/3 according to their statistical weights. For the case that the electron is captured into the 10s state, the cascade effect on n = 7 and 8 levels is quite large as shown in Fig.5(a). The contribution by cascades after charge exchange recombination is indicated by the hatched regions, and the region without hatching is the contribution of radiative recombination. Cascades following capture into the 10p state to the lower levels ($n \leq 9$) is very small, since the direct radiative transition from 10p to 1s is dominant (Fig.5(b)). For the case of capture into 10d, although the cascade is not so large as in the case of 10s due to the radiative transitions to the f states, the cascade is very effective(Fig.5(c)). Increasing the ℓ values with f, g, ..., the cascade effect decreases. For the capture into the levels with $\ell \geq 4$, the cascade contribution is negligibly small and the line emissions are dominated by radiative recombination as shown in Fig.5(e). Figs.5(f) and (g) show the results with the distribution of statistical weight like Ref.7 and with eq. (2), respectively. Cascades to the levels $n \leq 9$ are very small compared to the intensity from the transition from n = 10 for both cases.

We consider two extreme cases; (A) I_7 and I_8 are produced only by cascades from the n = 9 and 10 levels, and (B) I_7 and I_8 are produced mainly by direct capture to the p state.

Case (A); Most of the electrons captured to the 9ℓ or 10ℓ state flow to lower states(n = 1, 2, 3 etc) through direct radiative transitions and a few percent of electrons flow to the 7p state to produce I_7. Electron capture to the s states enhances I_7 and I_8 through cascades most effectively. This results in strong I_z as discussed in the next section(see Fig.7). The electron capture to the levels of larger ℓ values such as 9f and 9g is not efficient in producing the resonance series lines I_7 and I_8. The best candidate to enhance these lines is charge exchange to s and d states. We derive the values of the cross section in order to account for the measured intensities of I_7 and I_8 . The cross sections relative to that for the 10p state are obtained for (i) 10s, 9p and 9s states and (ii) 10d, 9p and 9d states. The resulting cross sections for the s and d states are larger by a factor of 5 and one order of magnitude respectively than that for the 10p state. A part of I_9 is ascribed to the direct capture to the 9p state through charge exchange. The relative cross sections thus derived are summarized as cases A(i) and A(ii) in Table I, and the resultant line intensities for I_7 through I_{10} are compared with the measurement in Fig.6, where T_e = 300 eV, N_e = 5 x 10^{13} cm^{-3}, $N(Ar^{17+})/N(Ar^{16+})$ = 0.02 and $N_H(1)$ = 8 x 10^8 cm^{-3} are assumed. The filled circles and triangles are the

results from the cases of A(i) and A(ii), respectively, and the measurements are indicated by the crosses. The contribution of radiative recombination is small compared to charge exchange recombination as indicated by open circles in Fig.6. The derived cross sections with the parameters mentioned above are shown in Fig.4 by circles.

Case (B); The intensities I_7 - I_{11} are dominated by direct capture to np states. The intensity difference between I_7 and I_8, however, is to be explained by cascades from n = 9 and 10. The cross sections deduced under this assumption are listed in Table I for two cases; (i) s and p states and (ii) p and d states. Calculated line intensities for (B) are not shown in Fig.6 since they are nearly the same as for (A).

The observed intensities I_7 and I_8 cannot be reproduced by the distribution given by Refs. 5, 7 and 8 because the cascade contribution to I_7 is too small. The calculated line intensities from the distribution by Koike[8] is shown by open triangles in Fig.6.

iv) Cascade effects on the spectra for the transitions of n = 2 to n = 1

The cascade contribution from the levels of large ℓ value such as d, f, g states enhances the intensity ratio $(I_x + I_y)/I_z$, whereas the cascades from the levels of small ℓ value such as s states reduces this ratio. With increasing ℓ values, the intensity ratio $(I_x + I_y) / I_w$ becomes smaller. In Fig.7

calculated intensities of I_w, I_x and I_y normalized to I_z are shown by solid lines for the cases of charge exchange to n = 10 state with only one of the levels of ℓ = 0, 1, 2, 3, 4, and 9. The results from radiative recombination only are indicated by circles for 300 eV. The observed values are also plotted as the dashed lines with the electron temperatures.[1,3] The spectra at high temperatures are from the central region of the plasma and are dominated mainly by electron impact excitation. The spectra, at lower temperatures below 350 eV, are considered to consist of the two components due to radiative and charge exchange recombination. It is seen from Fig.7 that as the temperature decreases, the intensities of w, x and y decrease. This may indicate the temperature dependence of the ℓ distribution of charge exchange processes. Capture to the levels ℓ = 3 is necessary to explain the observed intensity ratios of $(I_x + I_y)/I_z$ for 350 eV when they are compared to the values of the radiative recombination process only (open circles in Fig.7). The distribution ℓ = 0 or 1 is most probable for explaining the spectra at 100 eV and 250 eV. The calculated intensity ratios for the case of A(i) and A(ii) in Table I are shown in Fig.7 by filled circles and triangles. The observed spectrum of 250 eV can be roughly explained by these cross sections.

v) Spectra of the transitions with $n \geq 15$

The broad feature for $n \geq 15$ in Fig.3 is considered to be due to charge exchange between hydrogen atoms in excited states and Ar^{17+} .[2] The electrons are captured to the levels near n = 18, 27 and 36 by charge exchange with hydrogen in the n_i = 2, 3 and 4, respectively.[2,9] The ratios of the hydrogen density in these excited states to that in the ground state are estimated to be $N_H(n_i)/N_H(1)$ = 0.0034, 0.0017 and 0.00075 for n_i = 2, 3 and 4, respectively for T_e = 300 eV and $n_e = 5 \times 10^{13}$ cm^{-3}.[10]

Cascade effect of the different ℓ distributions from 18ℓ and 27ℓ states to the lower levels are shown in Fig.8 for (a) ℓ =0, (b)ℓ = 2, (c) ℓ = 3 and (d) statistical weight distribution. Here $\alpha_{cx}(18\ell) = 1.8 \times 10^{-7}$ and $\alpha_{cx}(27\ell) = 6.9 \times 10^{-8}$ cm^3 s^{-1} are assumed to see clearly the effect of the cascades. As we have seen in the previous section, cascades to the lower np states from $\ell \geq 2$ states are very small. For the statistical weight distribution, the cascade contribution is so small that the peaks of lines cannot be clearly observed.

Since the observed intensities I_{13} and I_{14} are considered to be produced mainly by radiative recombinaiton as discussed in Sec.3(ii), the contribution of cascades from higher levels is expected to be small for these lines. Then for the levels with $n \geq 15$ we assume that almost all of the electrons are captured to the ℓ = 1 state. Comparison of the calculated spectrum with the observed one is shown in Fig.9. The cross sections derived for $n \geq 15$ are listed in Table II. These cross sections are

roughly expressed in the form of a Gaussian distribution as $\sigma($ np $) = \sigma_0 \exp(-((n - n_0)/\Delta n)^2)$, where the values of σ_0 are 68 x $\sigma(10p)$, 180 x $\sigma(10p)$ and 160 x $\sigma(10p)$ and the values of Δn are 5, 6 and 8 for n_0 = 19, 27 and 36, respectively. The populations for the levels of $n > 27$ are re-distributed due to ℓ mixing. This effect is taken into account in our calculations. The spectral lines in Fig.9 are assumed to be emitted mainly at the plasma periphery near r = 13 cm where $T_e \approx 300$ eV, while continuum emission comes from the inner region where $T_e \approx 500$ eV. This plasma is considered to be in a low temperature recombining phase. The Boltzmann plot $N(n^1P)/(\omega(n^1P)n_e k)$ for the calculated population densities with the use of the charge exchange cross sections in Tables I and II is given in Fig.10 from n = 3 to 40 levels for T_e = 300 eV, $N_e = 5 \times 10^{13}$ cm^{-3} and $k = N(Ar^{17+})/N(Ar^{16+}) = 0.02$, where $N(n^1P)$ is the population density and ω the statistical weight. The population densities without charge exchange process and those in Saha-Boltzmann equilibrium are also shown by the dashed line and by the dot-dashed line, respectively. The population densities would be reached in local thermodynamic equilibrium at around n = 50. Strong population inversion is seen for the levels between n = 8 and 10 as well as between 13 and 27. The population densities for $n \geq 25$ exceed those of Saha- Boltzmann equilibrium.

4. Summary

Population inversion for n = 9, 10 and $\geq$ 15 states found from the peripheral region of tokamak plasmas has been analysed in terms of the charge exchange process. We have investigated the effect of cascades through charge exchange recombination and derived charge exchange cross sections to n - ℓ states for the process eq.(1) from the observed spectra. We considered the two extreme cases (A) and (B), and both fitted well to the experiment. We may assume that the actual distribution of the cross sections would be somewhere between case (A) and (B). The total cross section for n_i = 1 is 15 x σ(10p) in cases A(i) and B(i), 33 - 44 x σ(10p) in cases A(ii) and B(ii), respectively. These values are about the same as the theoretical ones given in Ref.6 taking the value σ(10p) = 4 x 10^{-16} cm^2. The total cross sections for n_i = 2, 3 and 4 are calculated to be 2.1 x 10^{-13}, 4.8 x 10^{-13} and 5.2 x 10^{-13} cm^2, respectively. This result indicates a weaker n_i dependence than that proportional to n_i^4. [2,9] The absolute values obtained in the present paper may be uncertain with an error of a factor of three depending on the uncertainties in v $N_H(1)/n_e$ in eq.(2).

There are few theoretical and experimental studies on n - ℓ distribution for highly ionized ions, particularly at low energies. The theoretical distributions [5,6,7,8] cannot reproduce the observed intensities from I_7 to I_{10} as mentioned in Sec. 3(iii). The ℓ distribution derived from the observed spectra appears to take a maximum around the s or d state for n

= 9 and 10. Since the maximum value in the s state of ℓ distribution (A(i) and B(i)) is difficult to be expected theoretically at low enegies, the second case in which the cross section increases towards the d state (A(ii) and B(ii)) would be more probable. The strong dependence on the temperature for the ℓ distribution may exist as discussed in Sec.3. The cross sections for the g state are unknown since the effect to the np states is small. The observed spectrum for $n \geq 15$ is consistent with the ℓ distribution having a maximum at the p state.

Acknowledgement

We would like to thank Prof. R. K. Janev for his useful comments.

References

1. E. Kallne, J. Kallne, A. Dalgarno, E.S. Marmar, J.E. Rice and A.K. Pradhan, Phys. Rev. Lett. 52, 2245 (1984)
2. J. E. Rice, E.S. Marmar, J.L. Terry, E. Kallne and J. Kallene, Phys. Rev. Lett. 56, 50 (1986)
3. J. E. Rice, E. S. Marmar, E. Kallne and J. Kallne, Phys. Rev. A 35, 3033 (1987)
4. T. Fujimoto and T. Kato, Astrophysical J. 246,994 (1981)
5. A. Abramov, F. F. Baryshnikov and V. S. Lisitsa, JETP Lett. 27, 464(1978)
6. R. K. Janev, D. S. Belic and B. H. Bransden, Phys. Rev. A, 28, 1293(1983)
7. W. Fritsch and H. Tawara, Phys. Scripta T28, 58(1989)
8. F. Koike, J. Phys. Soc. Japan, 57, 2344 (1988)
9. R. E. Olson, J. Phys. B, 13,483 (1980)
10. T. Fujimoto and P. McWhirter, Phys. Rev. A. Dec.1 (1990)

Table I

Relative charge exchange cross sections* for $Ar^{17+} + H(1) \rightarrow Ar^{16+}(n\,\ell) + H^+$

n =	7	8	9	10	Total
A(i)					
s			6.3	6.8	
p			0.95	1.1	
					14.6
A(ii)					
p			1.0	1.0	
d			21.0	21.0	
					44.0
B(i)					
s	2.1	4.3	4.3	2.1	
p	0.2	0.35	1.2	1.1	
					15.6
B(ii)					
p	0.3	0.35	1.2	1.0	
d	2.8	3.3	11.5	10.0	
					33.1

*normalized to $\sigma(10p) = 4.0 \times 10^{-16}$ cm^2 in the cases of A(ii) and B(ii)

Table II

Relative charge exchange cross sections*
for $Ar^{17+} + H(n_i) \rightarrow Ar^{16+}(n\,\ell) + H^+$ ($n_i \geq 2$ and $n \geq 15$)

$n_i = 2$		$n_i = 3$		$n_i = 4$	
15p	4.1(1)	24p	1.4(2)	32p	1.2(2)
16p	5.7(1)	25p	1.5(2)	33p	1.3(2)
17p	6.5(1)	26p	1.6(2)	34p	1.5(2)
18p	6.8(1)	27p	1.8(2)	35p	1.6(2)
19p	6.8(1)	28p	1.6(2)	36p	1.6(2)
20p	6.8(1)	29p	1.5(2)	37p	1.6(2)
21p	6.5(1)	30p	1.4(2)	38p	1.5(2)
22p	5.7(1)	31p	1.1(2)	39p	1.3(2)
23p	4.1(1)			40p	1.2(2)
Total	5.3(2)		1.2(3)		1.3(3)

*normalized to $\sigma(10p) = 4.0(-16)$ cm^2

$N_H(2)/N_H(1) = 3.4(-3)$, $N_H(3)/N_H(1) = 1.7(-3)$, $N_H(4)/N_H(1) = 7.5(-4)$

Figure captions

Fig.1 Observed spectra of $1s^2$ - $1s2\ell$ transitions in Ar^{16+} from Alcator-C tokamak for three different chords.[1]
w: $1s^2\ ^1S$ - $1s2p\ ^1P$, x: $1s^2$ - $1s2p\ ^3P_2$,
y: $1s^2\ ^1S$ - $1s2p\ ^3P_1$, z: $1s^2$ - $1s2s\ ^3S$

Fig.2 Observed spectra of $1s^2$ - 1snp transitions with $7 \leq n \leq 13$ in Ar^{16+} from Alcator-C tokamak for three different chords.[2]

Fig.3 Observed spectra of $1s^2$ - 1snp transitions with $n \geq 10$ in Ar^{16+} from Alcator-C tokamak.[2]

Fig.4 ℓ distribution of the cross section for the charge transferred electrons at low energies. Solid lines indicate the theoretical results by Koike[8] for Ar^{17+} + H at 0.35keV/amu, dashed lines from Fritsch and Tawara[7] for Si^{13+} + H at 0.35 keV/amu, dot - dashed line from Abramov[5] for A^{17+} + H at 0.5keV/amu. The derived distributions from the spectra are shown by open circles for case A(i) and by closed circles for A(ii), respectively. The ℓ distribution for the radiative recombination cross section of n = 10 levels is also shown in the upper part for comparison.

Fig.5 The calculated spectra for the transitions of n = 7 - 12 due to the charge transfer to the 10ℓ selected state are shown for a) 10s, b) 10p, c) 10d, d) 10f, e) 10g, respectively. The hatched regions indicate the contribution by charge exchange. The spectrum of (e) is the same as that from only radiative recombination. The spectra with the statistical weight distribution and eq.(2) are also shown in (f) and (g).

Fig.6 Line intensities for $1s^2$ - 1snp transitions with $7 \leq n \leq 10$. The filled circles and triangles are the calculated results for the case of A(i) and A(ii) in Table I. The crosses indicate the measurement at around 290 eV which corresponds to

Fig.2(c). The open circles show the contribution by rdiative recombination. The open triangles are the calculated intensities from the distribution of Ref.8. T_e = 350 eV, N_e = 5 x 10^{13} cm^{-3}, N_H = 10^9 cm^{-3} and $N(Ar^{17+})/N(Ar^{16+})$ = 0.02 are taken for calculations.

Fig.7 Intensity ratios of I_w, I_x and I_y to I_z. The solid lines are the calculated results assuming the charge exchange recombination to the 10ℓ state. Dashed lines are the observed values. The calculated ones by (o) radiative recombination only, (o) charge exchange recombination with the distribution in Table I A(i), (Δ) Table I A(ii).

Fig.8 Calculated spectra for $n \geq 10$ with different ℓ - distributions of the charge exchange cross sections of $\alpha_{cx}(18\ell) = 1.8 \times 10^{-7}$ and $\alpha_{cx}(27\ell) = 6.9 \times 10^{-8}$ $cm^3 s^{-1}$. (a) ℓ = 0, (b) ℓ = 2, (c) ℓ = 3 and (d) statistical weight.

Fig.9 Calculated spectrum (solid curve) and observed one (points) of $1s^2$ - $1sn\ell$ transitions with $n \geq 10$. The hatched regions show the contribution by radiative recombination.

Fig.10 Boltzman plot $N(n^1P)/(\omega(n^1P)n_e k)$ under the condition of N_e = 5 x 10^{13} cm^{-3}, T_e = 300 eV and k = $N(Ar^{17+})/N(Ar^{16+})$ = 0.02. The calculated one with the charge exchange cross sections in Table I and II is given by solid line. The dotted line and dot-dashed line show the results without charge exchange recombination and in the Saha - Boltzmann equilibrium, respectively.

Fig. 1

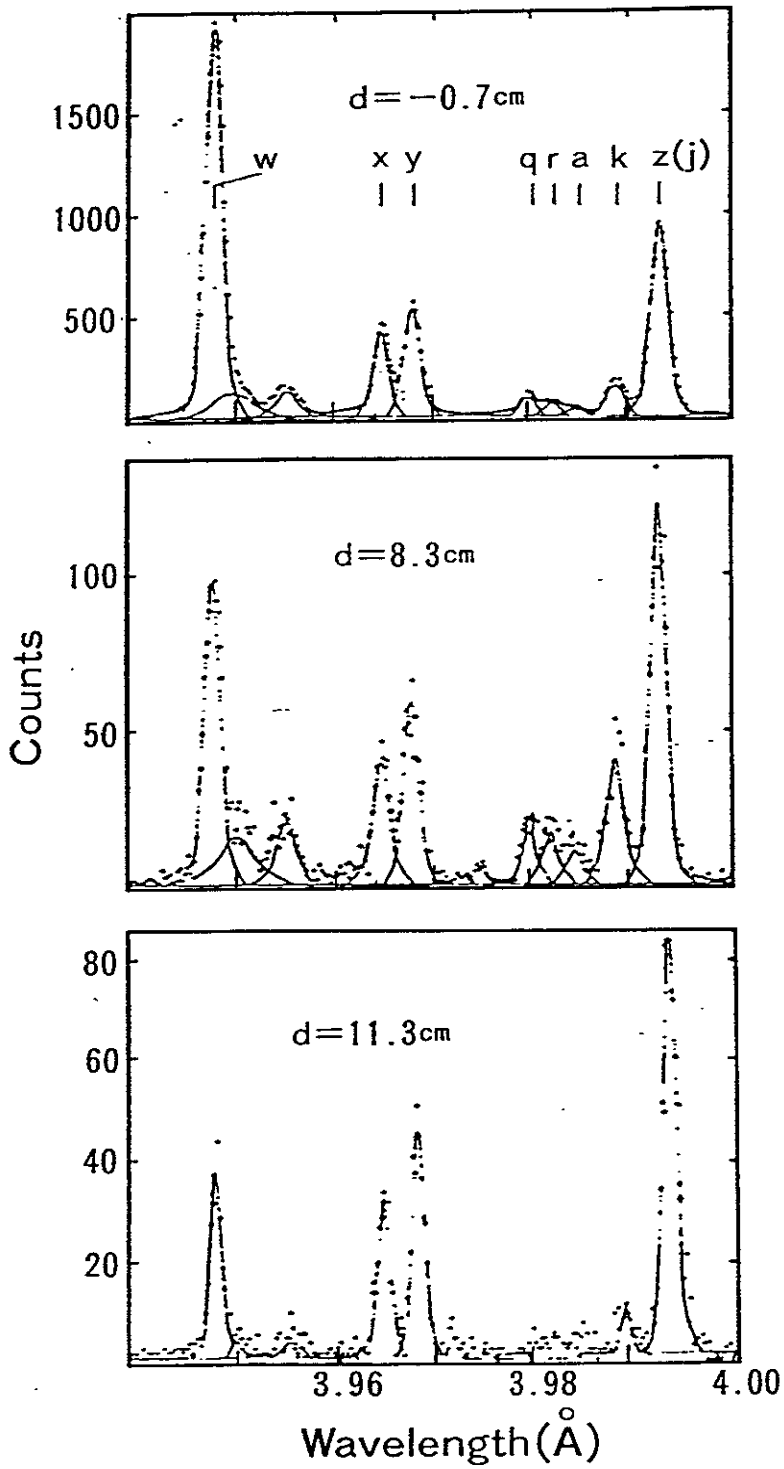
d=−0.7cm
w
x y
q r a k z(j)
1500
1000
500
d=8.3cm
100
50
Counts
d=11.3cm
80
60
40
20
3.96
3.98
4.00
Wavelength(Å)

Fig 2

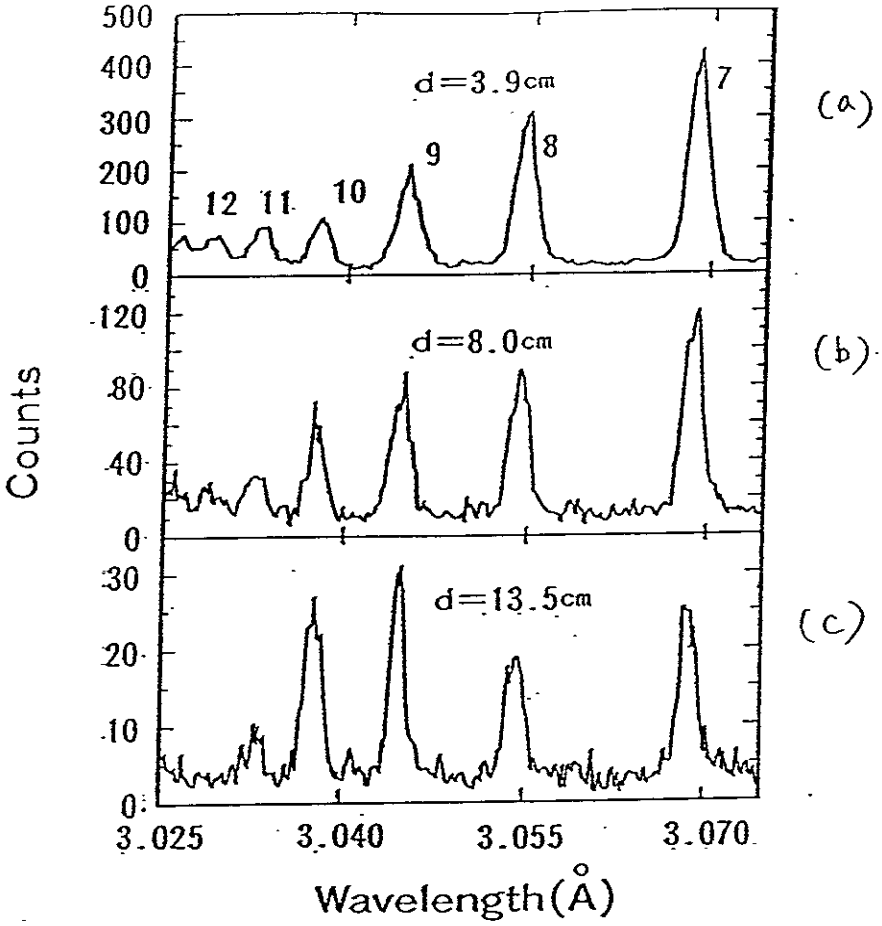
d=3.9cm
d=8.0cm
d=13.5cm
(a)
(b)
(c)
12
11
10
9
8
7
Counts
Wavelength(Å)
3.025
3.040
3.055
3.070

Fig 3

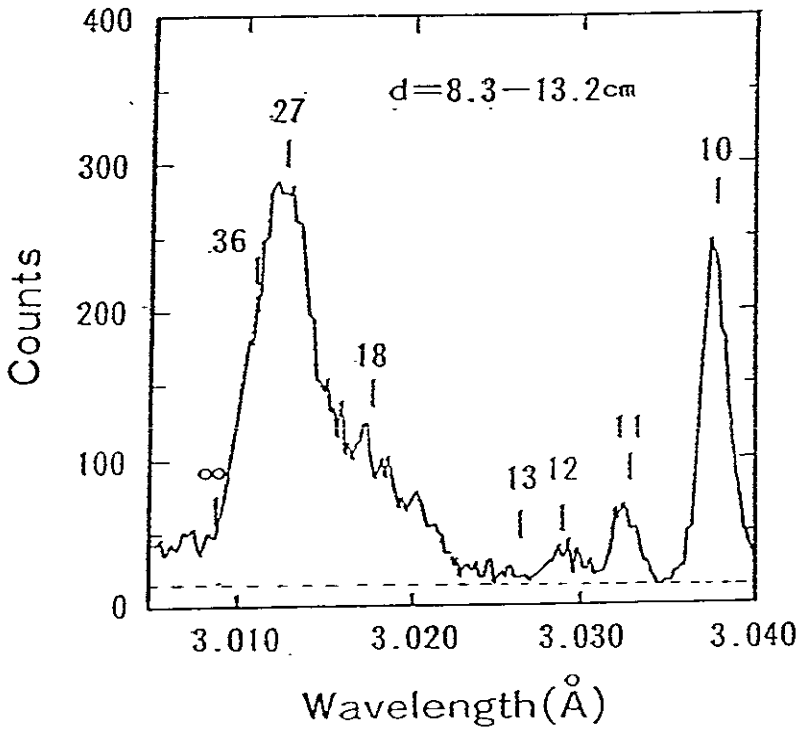
d=8.3—13.2cm
27
36
18
13
12
11
10
Counts
Wavelength(Å)
3.010
3.020
3.030
3.040

Fig. 4

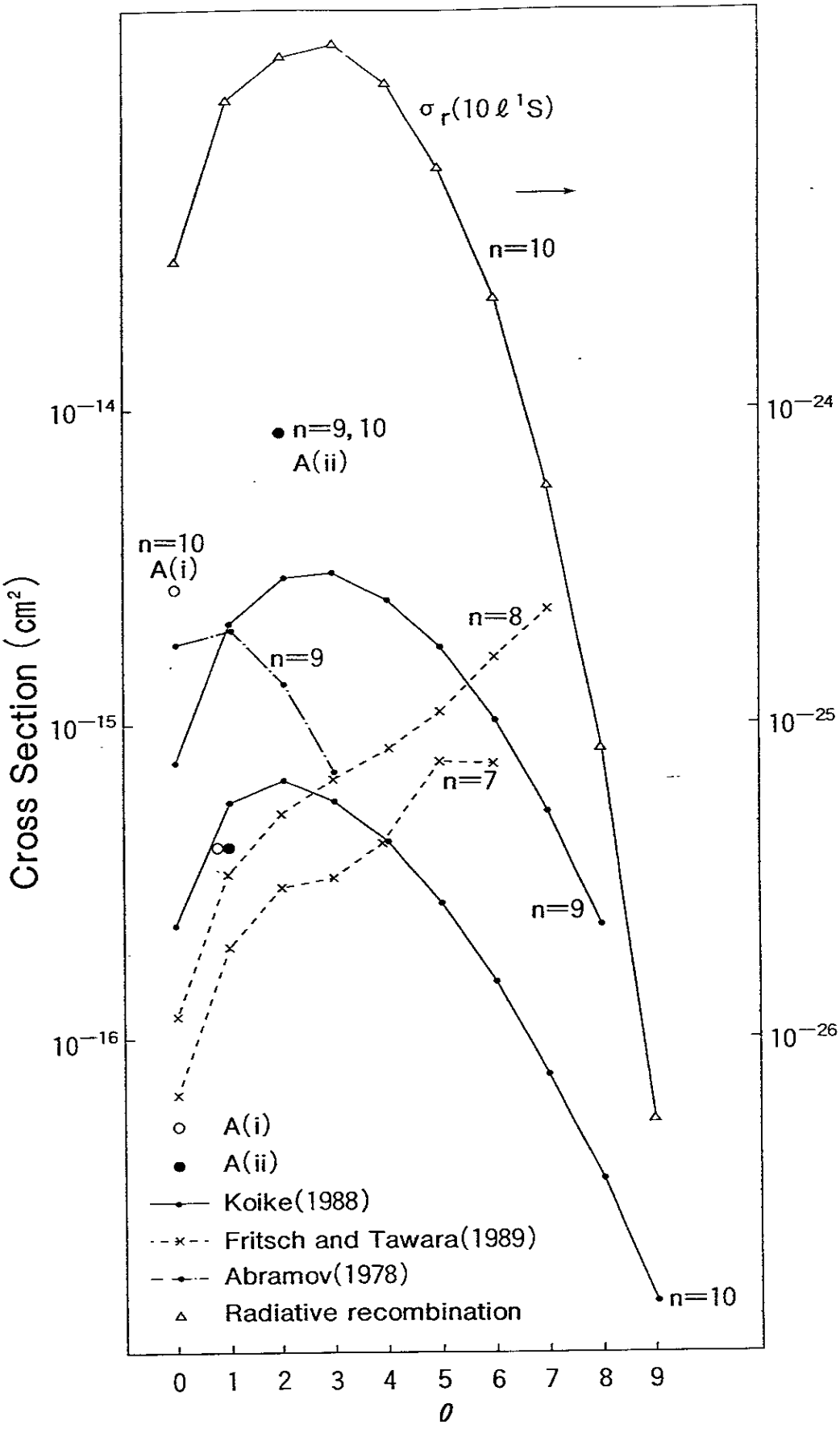
$\sigma_r(10\ell\ ^1S)$
n=10
n=9, 10
A(ii)
n=10
A(i)
n=8
n=9
n=7
n=9
n=10
10^{-14}
10^{-15}
10^{-16}
10^{-24}
10^{-25}
10^{-26}
Cross Section (cm^2)
A(i)
A(ii)
Koike(1988)
Fritsch and Tawara(1989)
Abramov(1978)
Radiative recombination
0 1 2 3 4 5 6 7 8 9
ℓ

Fig. 5

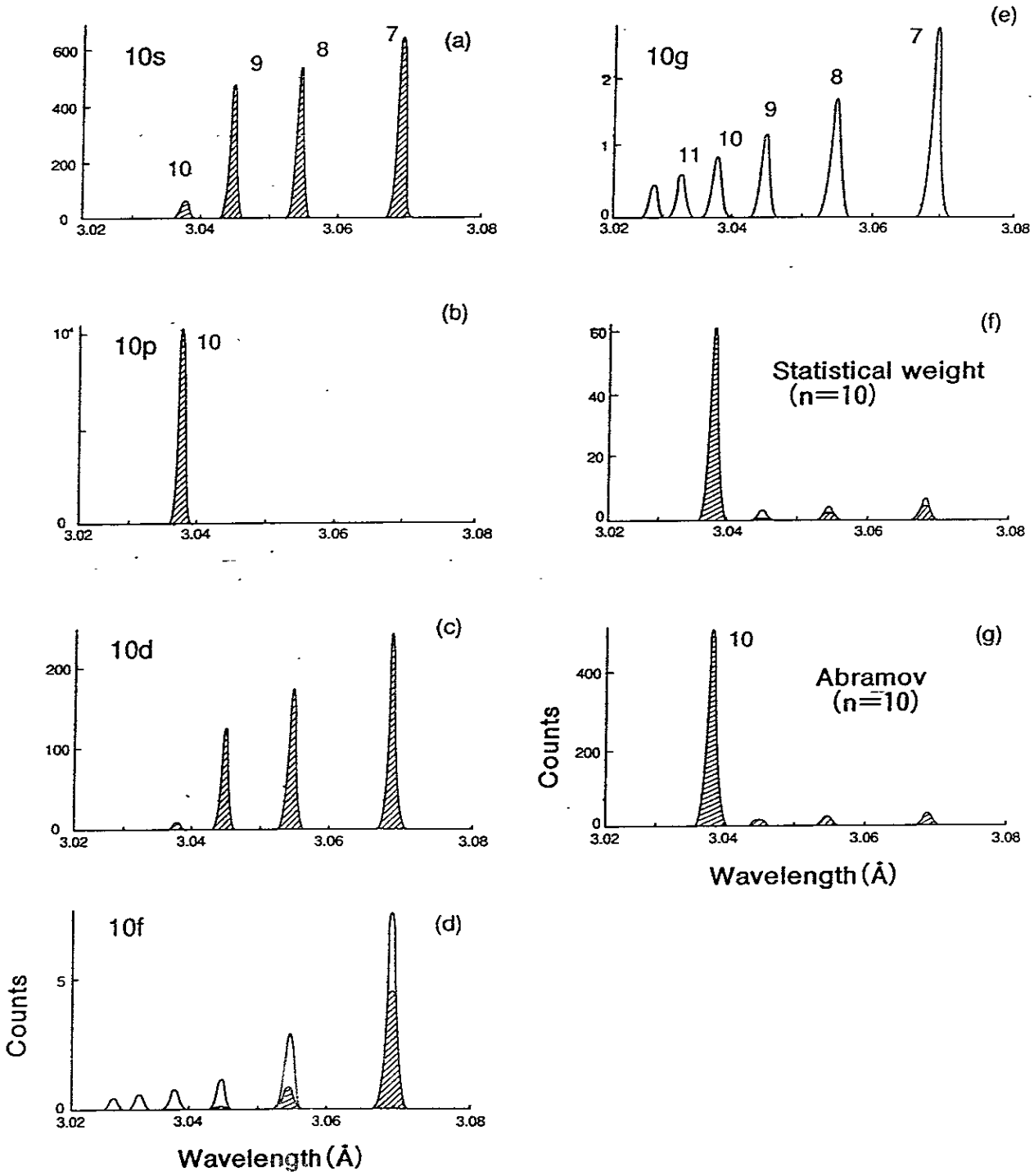
10s
(a)
10
9
8
7
600
400
200
0
3.02
3.04
3.06
3.08
10g
(e)
11
10
9
8
7
2
1
0
10p
(b)
10
10⁴
Statistical weight
(n=10)
(f)
60
40
20
10d
(c)
200
100
10f
(d)
5
Abramov
(n=10)
(g)
Counts
Wavelength (Å)

Fig. 6

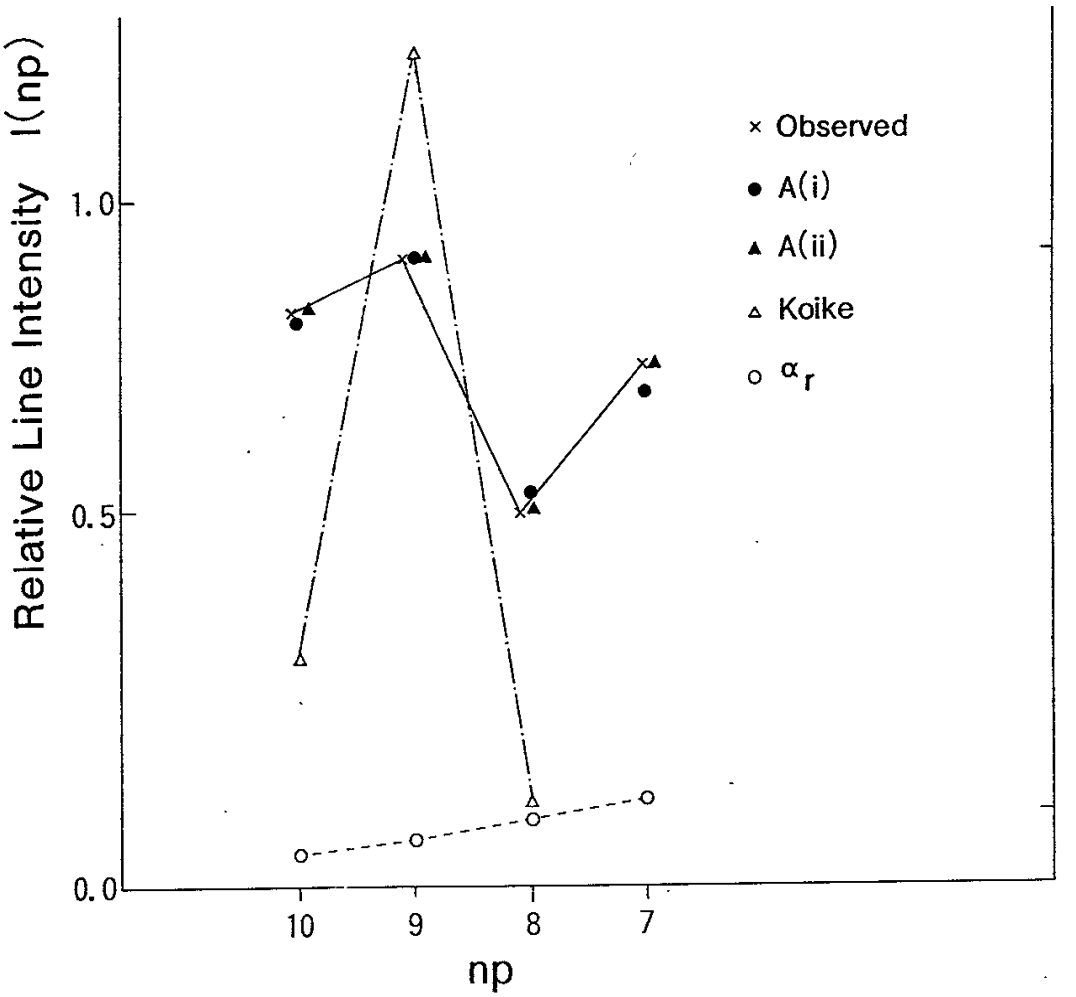
Relative Line Intensity I(np)
1.0
0.5
0.0
10
9
8
7
np
× Observed
● A(i)
▲ A(ii)
△ Koike
○ α_r

Fig. 7

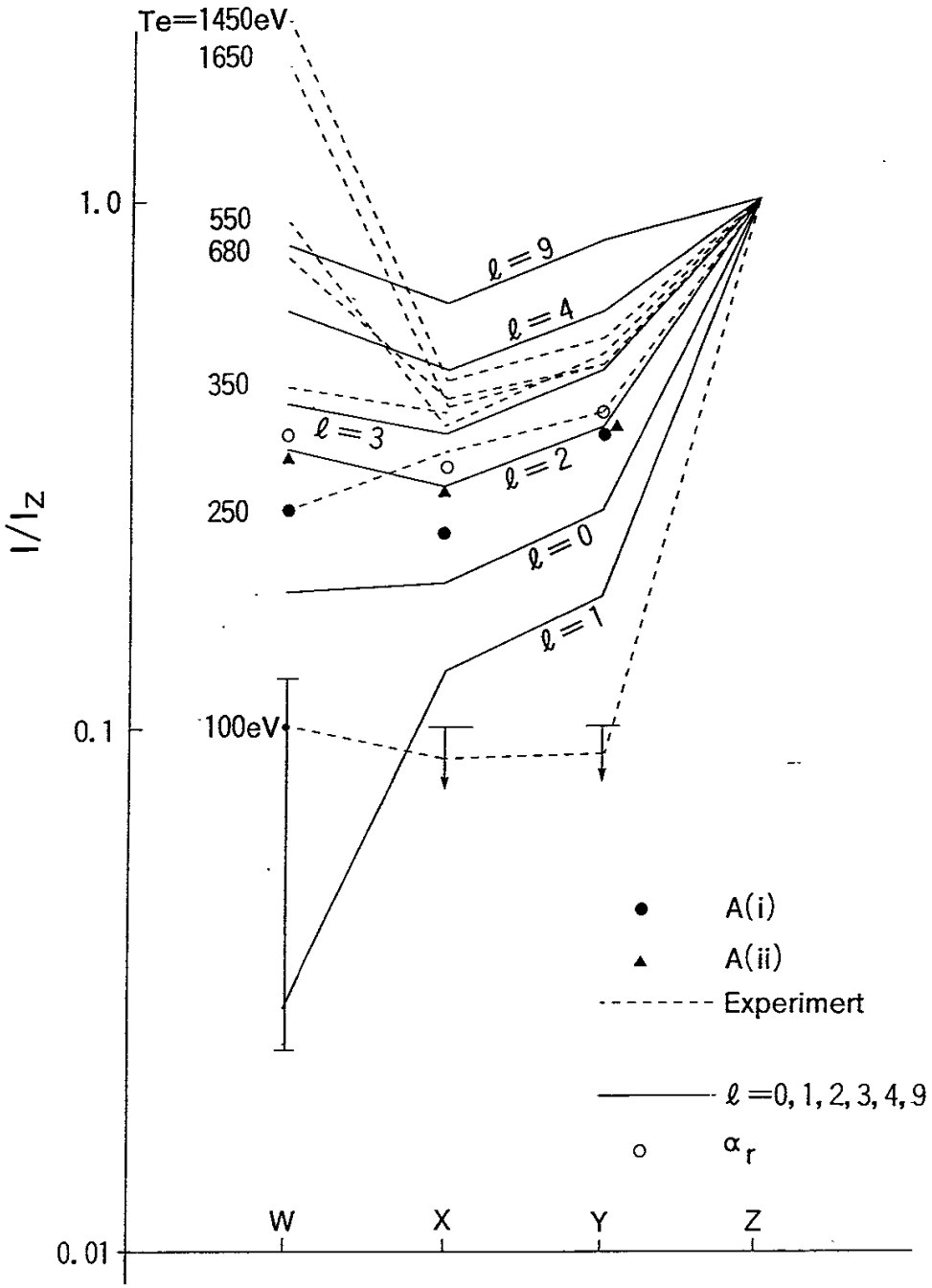
Te=1450eV
1650
1.0
550
680
350
250
0.1
100eV
0.01
I/I_Z
ℓ=9
ℓ=4
ℓ=3
ℓ=2
ℓ=0
ℓ=1
W
X
Y
Z
A(i)
A(ii)
Experimert
ℓ=0, 1, 2, 3, 4, 9
α_r

Fig. 8

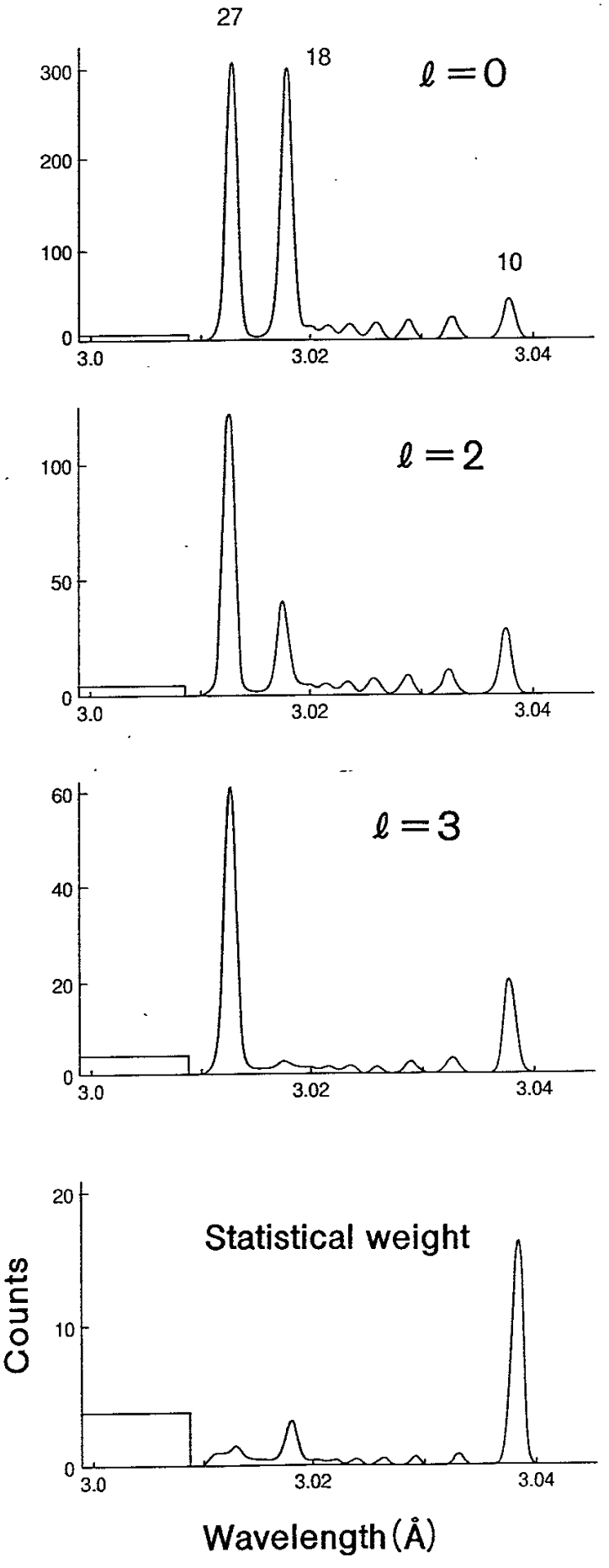
27
18
ℓ = 0
300
200
100
0
10
3.0
3.02
3.04
(a)
ℓ = 2
100
50
0
(b)
ℓ = 3
60
40
20
0
(c)
Statistical weight
Counts
20
10
0
(d)
Wavelength (Å)

Fig. 9

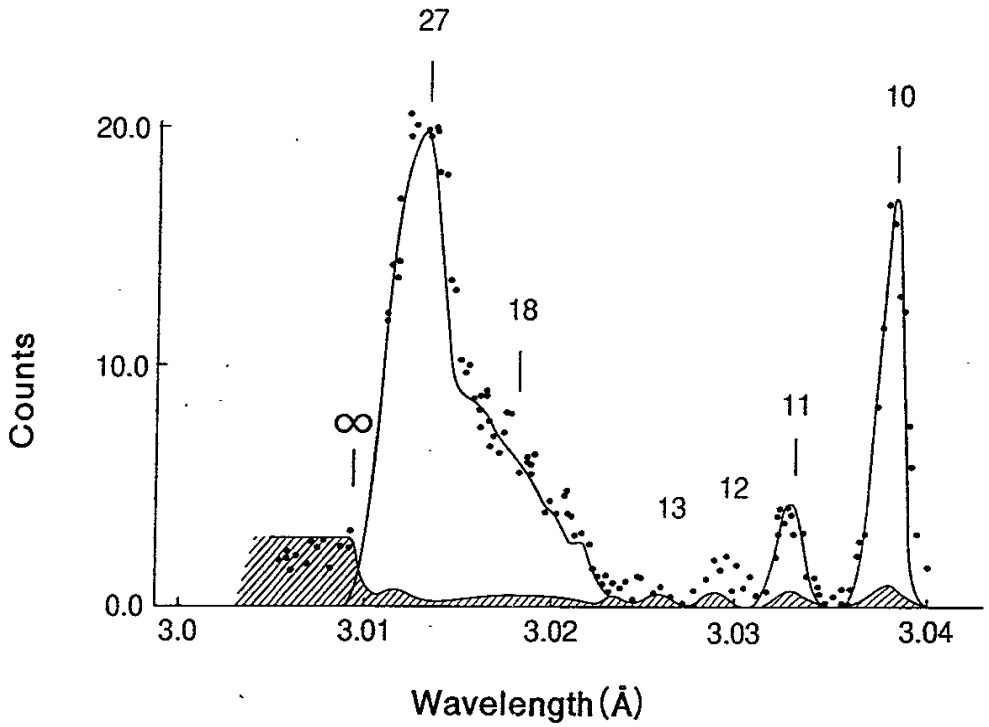
27
10
20.0
18
10.0
∞
11
13
12
0.0
3.0
3.01
3.02
3.03
3.04
Counts
Wavelength (Å)

Fig. 10

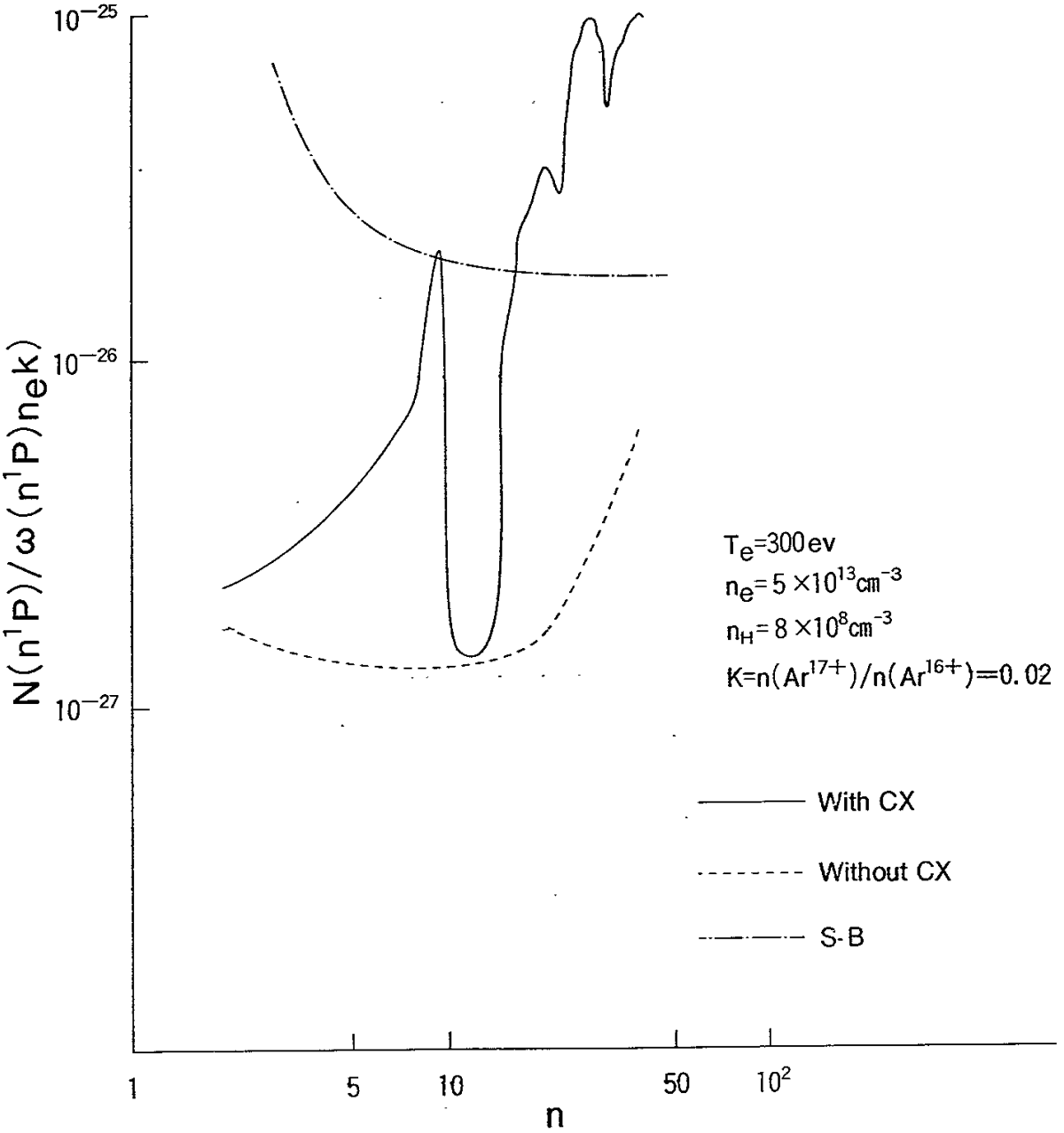
10^{-25}
10^{-26}
10^{-27}
$N(n^1P)/\omega(n^1P)n_e k)$
1
5
10
50
10^2
n
T_e=300ev
n_e=5 ×10^{13}cm^{-3}
n_H=8 ×10^8cm^{-3}
K=n(Ar^{17+})/n(Ar^{16+})=0.02
With CX
Without CX
S-B

Recent Issues of NIFS Series

NIFS-36 N. Ueda, S.-I. Itoh, M. Tanaka and K. Itoh, *A Design Method of Divertor in Tokamak Reactors* Aug. 1990

NIFS-37 J. Todoroki, *Theory of Longitudinal Adiabatic Invariant in the Helical Torus*; Aug. 1990

NIFS-38 S.-I. Itoh and K. Itoh, *Modelling of Improved Confinements – Peaked Profile Modes and H-Mode–* ; Sep. 1990

NIFS-39 O. Kaneko, S. Kubo, K. Nishimura, T. Syoji, M. Hosokawa, K. Ida, H. Idei, H. Iguchi, K. Matsuoka, S. Morita, N. Noda, S. Okamura, T. Ozaki, A. Sagara, H. Sanuki, C. Takahashi, Y. Takeiri, Y. Takita, K. Tsuzuki, H. Yamada, T. Amano, A. Ando, M. Fujiwara, K. Hanatani, A. Karita, T. Kohmoto, A. Komori, K. Masai, T. Morisaki, O. Motojima, N. Nakajima, Y. Oka, M. Okamoto, S. Sobhanian and J. Todoroki, *Confinement Characteristics of High Power Heated Plasma in CHS*; Sep. 1990

NIFS-40 K. Toi, Y. Hamada, K. Kawahata, T. Watari, A. Ando, K. Ida, S. Morita, R. Kumazawa, Y. Oka, K. Masai, M. Sakamoto, K. Adati, R. Akiyama, S. Hidekuma, S. Hirokura, O. Kaneko, A. Karita, T. Kawamoto, Y. Kawasumi, M. Kojima, T. Kuroda, K. Narihara, Y. Ogawa, K. Ohkubo, S. Okajima, T. Ozaki, M. Sasao, K. Sato, K.N. Sato, T. Seki, F. Shimpo, H. Takahashi, S. Tanahashi, Y. Taniguchi and T. Tsuzuki, *Study of Limiter H- and IOC- Modes by Control of Edge Magnetic Shear and Gas Puffing in the JIPP T-IIU Tokamak*; Sep. 1990

NIFS-41 K. Ida, K. Itoh, S.-I. Itoh, S. Hidekuma and JIPP T-IIU & CHS Group, *Comparison of Toroidal/Poloidal Rotation in CHS Heliotron/Torsatron and JIPP T-IIU Tokamak*; Sep .1990

NIFS-42 T.Watari, R.Kumazawa,T.Seki, A.Ando,Y.Oka, O.Kaneko, K.Adati, R.Ando, T.Aoki, R.Akiyama, Y.Hamada, S.Hidekuma, S.Hirokura, E.Kako, A.Karita, K.Kawahata, T.Kawamoto, Y.Kawasumi, S.Kitagawa, Y.Kitoh, M.Kojima, T. Kuroda, K.Masai, S.Morita, K.Narihara, Y.Ogawa, K.Ohkubo, S.Okajima, T.Ozaki, M.Sakamoto, M.Sasao, K.Sato, K.N.Sato, F.Shinbo, H.Takahashi, S.Tanahashi, Y.Taniguchi, K.Toi, T.Tsuzuki, Y.Takase, K.Yoshioka, S.Kinoshita, M.Abe, H.Fukumoto, K.Takeuchi, T.Okazaki and M.Ohtuka, *,Application of Intermediate Frequency Range Fast Wave to JIPP T-IIU and HT-2 Plasma*;
Sep. 1990

NIFS-43 K.Yamazaki, N.Ohyabu, M.Okamoto, T.Amano, J.Todoroki, Y.Ogawa, N.Nakajima, H.Akao, M.Asao, J.Fujita, Y.Hamada, T.Hayashi, T.Kamimura, H.Kaneko, T.Kuroda, S.Morimoto, N.Noda, T.Obiki, H.Sanuki, T.Sato, T.Satow, M.Wakatani, T.Watanabe, J.Yamamoto, O.Motojima, M.Fujiwara, A.Iiyoshi and LHD Design Group, *Physics Studies on Helical Confinement Configurations with l=2 Continuous Coil Systems*; Sep. 1990

NIFS-44 T.Hayashi, A.Takei, N.Ohyabu, T.Sato, M.Wakatani, H.Sugama, M.Yagi, K.Watanabe, B.G.Hong and W.Horton, *Equilibrium Beta Limit and Anomalous Transport Studies of Helical Systems*; Sep. 1990

NIFS-45 R.Horiuchi, T.Sato, and M.Tanaka, *Three-Dimensional Particle Simulation Study on Stabilization of the FRC Tilting Instability*; Sep. 1990

NIFS-46 K.Kusano, T.Tamano and T. Sato, *Simulation Study of Nonlinear Dynamics in Reversed-Field Pinch Configuration*; Sep. 1990

NIFS-47 Yoshi H.Ichikawa, *Solitons and Chaos in Plasma*; Sep. 1990

NIFS-48 T.Seki, R.Kumazawa, Y.Takase, A.Fukuyama, T.Watari, A.Ando, Y.Oka, O.Kaneko, K.Adati, R.Akiyama, R.Ando, T.Aoki, Y.Hamada, S.Hidekuma, S.Hirokura, K.Ida, K.Itoh, S.-I.Itoh, E.Kako, A. Karita, K.Kawahata, T.Kawamoto, Y.Kawasumi, S.Kitagawa, Y.Kitoh, M.Kojima, T.Kuroda, K.Masai, S.Morita, K.Narihara, Y.Ogawa, K.Ohkubo, S.Okajima, T.Ozaki, M.Sakamoto, M.Sasao, K.Sato, K.N.Sato, F.Shinbo, H.Takahashi, S.Tanahashi, Y.Taniguchi, K.Toi and T.Tsuzuki, *Application of Intermediate Frequency Range Fast Wave to JIPP T-IIU Plasma*; Sep.1990

NIFS-49 A.Kageyama, K.Watanabe and T.Sato, *Global Simulation of the Magnetosphere with a Long Tail: The Formation and Ejection of Plasmoids*; Sep.1990

NIFS-50 S.Koide, *3-Dimensional Simulation of Dynamo Effect of Reversed Field Pinch*; Sep. 1990

NIFS-51 O.Motojima, K. Akaishi, M.Asao, K.Fujii, J.Fujita, T.Hino, Y.Hamada, H.Kaneko, S.Kitagawa, Y.Kubota, T.Kuroda, T.Mito, S.Morimoto, N.Noda, Y.Ogawa, I.Ohtake, N.Ohyabu, A.Sagara, T. Satow, K.Takahata, M.Takeo, S.Tanahashi, T.Tsuzuki, S.Yamada, J.Yamamoto, K.Yamazaki, N.Yanagi, H.Yonezu, M.Fujiwara, A.Iiyoshi and LHD Design Group, *Engineering Design Study of Superconducting Large Helical Device*; Sep. 1990

NIFS-52 T.Sato, R.Horiuchi, K. Watanabe, T. Hayashi and K.Kusano, *Self-Organizing Magnetohydrodynamic Plasma*; Sep. 1990

NIFS-53 M.Okamoto and N.Nakajima, *Bootstrap Currents in Stellarators and Tokamaks*; Sep. 1990

NIFS-54 K.Itoh and S.-I.Itoh, *Peaked-Density Profile Mode and Improved Confinement in Helical Systems*; Oct. 1990

NIFS-55 Y.Ueda, T.Enomoto and H.B.Stewart, *Chaotic Transients and Fractal Structures Governing Coupled Swing Dynamics*; Oct. 1990

NIFS-56 H.B.Stewart and Y.Ueda, *Catastrophes with Indeterminate Outcome*; Oct. 1990

NIFS-57 S.-I.Itoh, H.Maeda and Y.Miura, *Improved Modes and the Evaluation of Confinement Improvement*; Oct. 1990

NIFS-58 H.Maeda and S.-I.Itoh, *The Significance of Medium- or Small-size Devices in Fusion Research*; Oct. 1990

NIFS-59 A.Fukuyama, S.-I.Itoh, K.Itoh, K.Hamamatsu, V.S.Chan, S.C.Chiu, R.L.Miller and T.Ohkawa, *Nonresonant Current Drive by RF Helicity Injection*; Oct. 1990

NIFS-60 K.Ida, H.Yamada, H.Iguchi, S.Hidekuma, H.Sanuki, K.Yamazaki and CHS Group, *Electric Field Profile of CHS Heliotron/Torsatron Plasma with Tangential Neutral Beam Injection*; Oct. 1990

NIFS-61 T.Yabe and H.Hoshino, *Two- and Three-Dimensional Behavior of Rayleigh-Taylor and Kelvin-Helmholz Instabilities*; Oct. 1990

NIFS-62 H.B. Stewart, *Application of Fixed Point Theory to Chaotic Attractors of Forced Oscillators;* Nov. 1990

NIFS-63 K.Konn., M.Mituhashi, Yoshi H.Ichikawa,*Soliton on Thin Vortex Filament;* Dec. 1990

NIFS-64 K.Itoh, S.-I.Itoh and A.Fukuyama,*Impact of Improved Confinement on Fusion Research;* Dec. 1990

NIFS -65 A.Fukuyama, S.-I.Itoh and K. Itoh,*A Consistency Analysis on the Tokamak Reactor Plasmas;* Dec. 1990

NIFS-66 K.Itoh, H. Sanuki, S.-I. Itoh and K. Tani,*Effect of Radial Electric Field on α-Particle Loss in Tokamaks;* Dec. 1990

NIFS-67 K.Sato,and F.Miyawaki,*Effects of a Nonuniform Open Magnetic Field on the Plasma Presheath*; Jan.1990

NIFS-68 K.Itoh and S.-I.Itoh,*On Relation between Local Transport Coefficient and Global Confinement Scaling Law;* Jan. 1991

NIFS DATA-1 Y. Yamamura, T. Takiguchi and H. Tawara, *Data Compilation of Angular Distributions of Sputtered Atoms* ; Jan. 1990

NIFS DATA-2 T. Kato, J. Lang and K. E. Berrington, *Intensity Ratios of Emission Lines from OV Ions for Temperature and Density Diagnostics* ; Mar. 1990

NIFS DATA-3 T. Kaneko, *Partial Electronic Straggling Cross Sections of Atoms for Protons* ; Mar. 1990

NIFS DATA-4 T. Fujimoto, K. Sawada and K. Takahata, *Cross Section for Production of Excited Hydrogen Atoms Following Dissociative Excitation of Molecular Hydrogen by Electron Impact* ; Mar. 1990

NIFS DATA-5 H. Tawara, *Some Electron Detachment Data for H- Ions in Collisions with Electrons, Ions, Atoms and Molecules – an Alternative Approach to High Energy Neutral Beam Production for Plasma Heating–* ; Apr. 1990

NIFS DATA-6 H. Tawara, Y. Itikawa, H. Nishimura, H. Tanaka and Y. Nakamura, *Collision Data Involving Hydro-Carbon Molecules* ; July 1990

NIFS DATA-7 H.Tawara, *Bibliography on Electron Transfer Processes in Ion-Ion/Atom/Molecule Collisions –Updated 1990–*; Oct. 1990

NIFS DATA-8 U.I.Safronova, T.Kato, K.Masai, L.A.Vainshtain and A.S.Shlyapzeva, *Excitation Collision Sterengths, Cross Scetions and Rate Coefficients for OV, SiXI, FeXXIII, MoXXXIX by Electron Impact($1s^2 2s^2$-$1s^2 2s2p$-$1s^2 2p^2$ Transitions)*

NIFS DATA-9 T.Kaneko, *Partial and Total Electronic Stopping Cross Sections of Atoms and Solids for Protons;* Dec 1990

NIFS TECH-1 H. Bolt and A. Miyahara, *Runaway–Electron –Materials Interaction Studies* ; Mar. 1990

NIFS PROC-1 *U.S.-Japan Workshop on Comparison of Theoretical and Experimental Transport in Toroidal Systems Oct. 23-27, 1989* ; Mar. 1990

NIFS PROC-2 *Structures in Confined Plasmas –Proceedings of Workshop of US-Japan Joint Institute for Fusion Theory Program–* ; Mar. 1990

NIFS PROC-3 *Proceedings of the First International Toki Conference on Plasma Physics and Controlled Nuclear Fusion –Next Generation Experiments in Helical Systems– Dec. 4-7, 1989* ; Mar. 1990

NIFS PROC-4 *Plasma Spectroscopy and Atomic Processes –Proceedings of the Workshop at Data & Planning Center in NIFS–*; Sep. 1990

NIFS PROC-5 *Symposium on Development of Intensed Pulsed Particle Beams and Its Applications*; Oct. 1990